In-Vivo Tests of a 16-Channel Implantable Wireless Neural Stimulator*

Philip Troyk[1], Samuel Bredeson[1], Stuart Cogan[2], Mario Romero-Ortega[2], Sungjae Suh[1], Zhe Hu[3], Aswini Kanneganti[2], Rafael Granja-Vazquez[2], Jennifer Seifert[2], Martin Bak[4]

***Abstract*— Wireless stimulation of neural tissue could enable many emerging neural prosthesis designs, and eliminate problems associated with percutaneous wires and connectors. Our laboratory has developed a 16-channel wireless floating microelectrode array (WFMA) for chronic implantation. Here, we report on its first use within in-vivo experiments, using a rat sciatic nerve model. Stimulus currents and associated muscular movements were determined for electrodes of two WFMA devices implanted into four animal subjects.**

I. INTRODUCTION

Wireless stimulation of the central and peripheral nervous system has been a goal of neural prosthesis developers for many years, and while technology has been reported that might be matured into a fully integrated multichannel wireless stimulation device by [1], [2], [3], and others, these have not resulted in the deployment or demonstration of a miniature, implantable, wireless, multichannel stimulator that uses microelectrodes to stimulate cortical neurons, or peripheral nerves.

For more than a decade, research work within the Laboratory of Neural Prosthetic Research at the Illinois Institute of Technology has been directed towards the development of a fully implantable 16-channel wireless stimulator module for use in an intracortical visual prosthesis [4], [5]. As part of that work, various technological approaches for driving activated iridium oxide film (AIROF) electrodes [6], [7], designing application-specific-integrated circuits [8], optimizing inductive links [9], and choosing power/communication strategies [10] have been matured. Recently, fabrication methodologies that demonstrate the robustness of non-hermetic packaging techniques suitable for chronic implantation have been reported [11]. The combination of these fundamental technologies has resulted in the testing of an implantable, wireless, 16-channel, AIROF microelectrode stimulator based upon Floating Microelectrode Array technology [12] suitable for implantation within the cortex and for incorporation into peripheral nerve cuffs. Here, we report on the first preliminary testing of the Wireless Floating Microelectrode Array (WFMA) in acute and chronic rat models.

*WFMA development supported by the Telemedicine and Advanced Technology Research Center, U.S. Army Medical Research and Material Command, Contract W81XWH-12-1-0394.

[1] Department of Biomedical Engineering, Illinois Institute of Technology, Chicago, IL (email: sam.bredeson@hawk.iit.edu).

[2] Department of Biomedical Engineering, University of Texas at Dallas.

[3] Sigenics, Inc., Chicago, IL.

[4] MicroProbes for Life Science, Gaithersburg, MD.

II. STIMULATOR TECHNOLOGY

As first reported in [5], [8], [10], the WFMA, as shown in Figure 1 is physically comprised of a ceramic platform that maintains the lateral position of eighteen (16 + reference + counter) Parylene- insulated microelectrodes and provides an interconnection substrate between a superstructure that contains an ASIC and microcoil, to form a fully integrated wireless stimulator module. The electrode tips are individually exposed by laser ablation of the Parlyene.

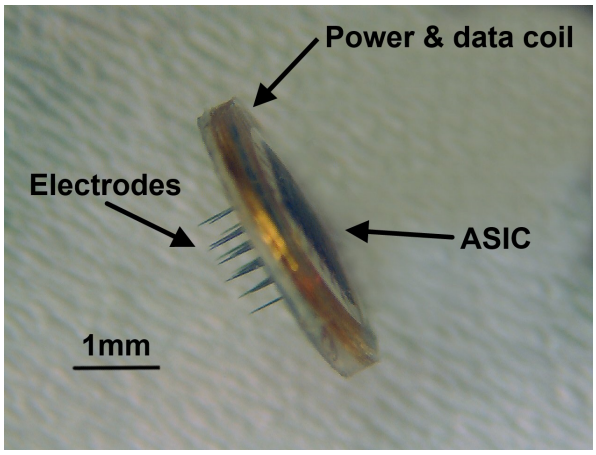

Fig. 1. Wireless floating microelectrode array (WFMA) used in this study.

The ASIC contains all required circuity for power rectification and management, bidirectional communication, state-machine command processing, sixteen individual AIROF electrode drivers, and housekeeping support. These circuits allow for receiving wireless power, processing wireless stimulation commands, providing constant-current charge-balanced electrode driving, and sending reverse telemetry of electrode voltage waveforms. In addition, specialized control of the ASIC permits activation of the iridium electrodes over the wireless inductive link [6], which is necessary to accommodate the high sealing temperatures of the polymer-based packaging methods. The inductive link uses a gold-wire microcoil as reported in [9]. At a current level of about one-ampere peak, for a transmitter frequency of 5MHz, power can be provided to the WFMA with about 3cm of separation between extracorporeal telemetry control unit (TC) and the WFMA. We anticipate approximately 4cm of separation distance will be feasible when using 1.5A peak. No components external to the ASIC are required. The ASIC contains a total of 2.5nF of power supply capacitance to stabilize the main and counter electrode supplies.

Forward command telemetry of the WFMA is provided using FSK-modulation of the Class-E converter in the TC [10], with a data rate of 1.2Mbits/second, using the NeuroTalk interface [8]. WFMAs are configured for random addressing of 16 microelectrodes, and up to 63 separate WFMAs can be individually addressed by one TC-controlled system for a possible system total of 1008 electrodes.

Each electrode has an independently-controlled constant current cathodic-first driver that uses potentiostatic control of the electrode voltage with respect to a non-current-carrying Pt-Ir reference electrode contained within the electrode cluster of the WFMA. Electrode current flows between the micro-(working) electrode and a counter electrode, using either compliance-supplied limited driving [8], that unconditionally maintains the electrodes within the water window, or a 4V compliance supply range, for a maximum of 63.5μA with 0.5μA steps. Pulse width can be controlled over the range of 0 - 400μsec with 15 steps. The driving circuitry is configured for biasing of the AIROF electrodes, to enhance, and optimize, the injectable charge capacity [7].

Monitoring of the electrode voltage during stimulation pulses is provided by a low-bandwidth reverse telemetry channel, operating on a 145kHz carrier. For each stimulation pulse, one sample of the electrode voltage and the reference voltage, can be telemetered. By changing the temporal location of the sample within the stimulation pulse for successive pulses, a composite stimulation voltage waveform can be constructed. The stimulation voltage waveforms yield valuable information about electrode polarization and safe electrode operation.

The TC unit contains an FSK-modulated, closed-loop Class-E converter [12], and the reverse telemetry receiver. Commands to the converter are processed by a combination of a dedicated FPGA fed by a data stream from a USB-processor module. Control of the TC is done using a graphical user interface on a PC that sends commands to the TC over the USB. Received data from the TC is processed and saved within CSV-format files for display and analysis.

Packaging of the WFMA uses silane-enhanced PDMS encapsulation. Overall package dimensions without electrodes are: 5mm diameter by 0.5mm thick. Accelerated testing of the WFMA packaging has been recently reported in [11], showing data from over 170 days of continuous biased operation within an autoclave at 121°C, 100% RH and 20psig, and ongoing testing has exceeded 250 days.

III. DEVICES

Three WFMA devices were constructed for use in in-vivo testing. The ceramic substrates with electrodes were manufactured by MicroProbes for Life Sciences and sent to the Illinois Institute of Technology. There, the WFMA device assembly was completed and the electrodes were wirelessly activated. The assembled devices were then returned to MicroProbes for mounting in silicone nerve cuffs.

To investigate neuron selectivity, four electrode tip exposure areas were selected, as well as two electrode lengths. These combined to yield eight different electrode configurations within the array. The four tip areas used were 500, 1000, 1500, and 2000μm^2 and the two electrode lengths were 500 and 700μm. Figure 2 shows a graphical represenation of the array layout, including electrode variations and positions. The reference and counter were uninsulated and 700μm long.

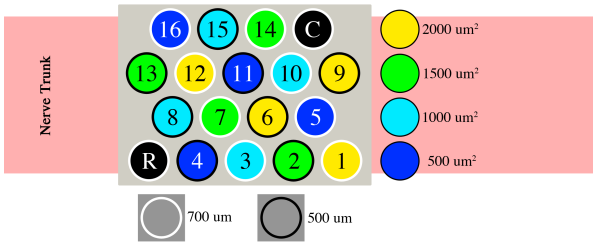

Fig. 2. Electrode array layout showing arrangement of the four electrode tip exposure areas and two electrode lengths used in this study. This view is from the substrate down (electrode tips into the page). The numbers indicate electrode ID numbers. R and C represent the reference and counter electrodes, respectively. The nerve trunk runs left to right or vice versa.

To facilitate the implantation of these devices into peripheral nerves. The cuffs were designed to straddle the nerve, improving alignment and mechanical stability. Figure 3 shows a completed WFMA device before implantation.

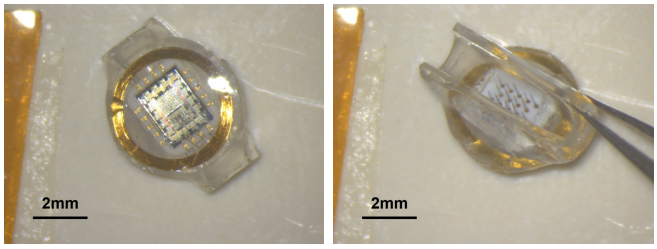

Fig. 3. Wireless stimulation device before implantation. Left: top view showing ASIC and coil. Right: bottom view showing electrodes and silicone nerve cuff.

Following O_2 plasma cleaning, all sixteen electrodes of each array were activated to grow the AIROF by cycling between -0.7V and +0.8V wrt Ag—AgCl for 200 cycles. Figure 4 shows a typical electrode before and after the activation process.

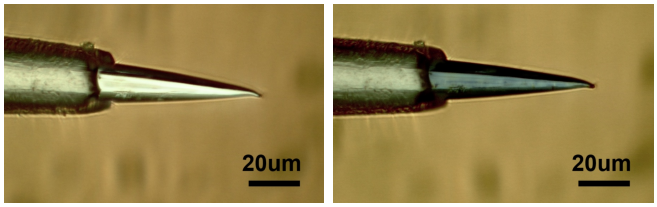

Fig. 4. A representative electrode shown before (left) and after (right) 200 cycles of activation.

IV. IN-VITRO CHARACTERIZATION

Before implantation, the electrodes were characterized in-vitro to determine their relative performance levels and to confirm that they were properly activated. Each device was

placed in phosphate-buffered saline and the waveforms of each electrode were observed during pulsing. A typical in-vitro waveform is shown in Figure 5. Obvious data transmission errors were removed, then a rolling average (N=10) was applied to the difference waveform to smooth the data.

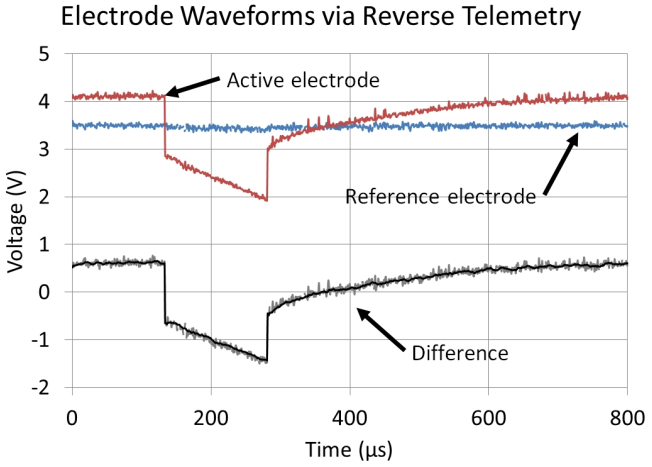

Fig. 5. A representative waveform recorded during in-vitro characterization of the electrodes. Waveform noise was caused by data transmission via the reverse telemetry.

V. IN-VIVO EXPERIMENTS

To examine the ability of the devices to stimulate neural tissue, two of the WFMAs were implanted onto female Lewis rat sciatic nerves. First, array A was implanted into two acute animals, then arrays A and B were implanted into two different animals for a chronic study - chronic testing to be reported in a future publication. Array C was reserved for future testing.

A. Surgical procedure

As approved by the animal welfare community at UTD: Under inhaled 2% Isoflurane anesthesia and sterile conditions, the rat's left lateral hind limb received a 4cm incision following the femur from knee to hip as an underlying landmark. The skin was separated by blunt dissection from the underlying muscular fascia. A longitudinal incision was made in the fascia between the biceps femoris and quadriceps femoris muscles and the sciatic nerve was exposed. Using 25x magnification, the sciatic nerve was dissected free from surrounding tissue leaving a 2cm section for interfacing with the WFMA, as shown in Figure 6. The nerve was inserted into the cuff with gentle manual pressure. Full limb flexion and extension was used to confirm the mechanical robustness of the interface to the nerve. The muscular fascia was closed with a single point 4-0 chromic gut, and the skin was affronted with stainless steel staples followed by the application of a triple antibiotic ointment.

All animals received corresponding post-operative care that included monitoring and administration of an analgesic (buprenorphine SC) and prophylactic antibiotic (cefazolin IM).

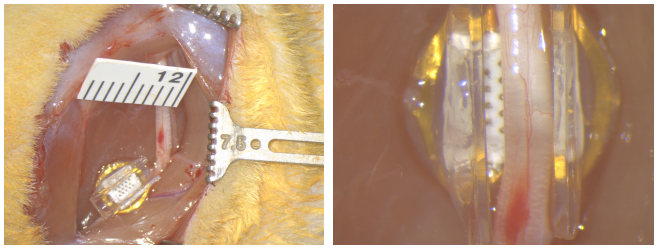

Fig. 6. Array A during the implantation procedure. Left: implant location being prepared and size of nerve determined (scale in mm). Right: nerve positioned above electrode array, demonstrating mismatch between array and nerve width.

B. Threshold detection

Each electrode was pulsed individually to determine the threshold current for producing a muscle response. A biphasic pulse was applied with a 200μs square-wave cathodic-first pulse at a frequency of 2Hz. Cathodic current was adjusted to locate the muscle threshold, beginning at either 5 or 10μA. Muscle threshold was defined as the smallest current level that produced a visible muscle twitch. The current and movement type were recorded for each electrode.

VI. RESULTS

Muscle responses were observed across a large number of the implanted electrodes. The four implantations (three for Array A and one for Array B) had 9, 13, 9, and 13 functional electrodes, respectively. Among the three implantations of Array A, several electrodes showed a repsonse in at least one animal while showing no response in another, indicating that the lack of function seen in some electrodes was due to variations due to electrode placement relative to the nerve rather than an electrical or mechanical failure of the electrode in question. Only three electrodes on Array A showed no muscle response in any of the animals: 9, 11, and 15.

If a muscle threshold was present for a given electrode, several higher levels of current were tested to determine if the strength or type of muscle response could be controlled. As expected, it was observed that an increase in current resulted in a stronger muscle response. Additional current also often caused a change in movement type, although the general direction of movement tended to be consistent. For example, if threshold current produced digit flexion, increasing current may have caused a plantar flexion movement, but was unlikely to produce dorsiflexion. Table I lists the threshold and maximum current levels used on each electrode, as well as the movement type and strength seen at that current.

In vivo, commands and reverse telemetry were successfully sent across the transcutaneous link with the transmission coils up to 2cm away from the animals' skin, as shown in Figure 7. The implants were positioned approximately 1cm below the skin in all four animals, yielding a total transmission distance of up to 3cm.

VII. DISCUSSION AND CONCLUSIONS

These in-vivo experiments, using the WFMA demonstrate the feasibility of incorporating a multichannel wireless mi-

TABLE I

THRESHOLD (THRESH) AND MAXIMUM (MAX) CURRENTS REQUIRED TO PRODUCE MUSCULAR RESPONSES. (CURRENTS IN MICROAMPERES.)

	Array A - Acute 1				Array A - Acute 2			
El.	Thresh	Mov	Max	Mov	Thresh	Mov	Max	Mov
1	11.0	a tf	20.0	A p	5.0	tf	7.5	A P
2	-	-	20.0	-	15.0	te	20.0	D
3	10.0	tf	15.0	D	5.0	tf	15.0	P
4	-	-	20.0	-	15.0	te	20.0	D
5	-	-	20.0	-	3.5	tf	7.5	a P
6	-	-	15.0	-	15.0	tf	20.0	P
7	10.0	tf	20.0	A P	5.0	tf	7.5	A P
8	10.0	te	20.0	A d	2.5	tf	7.5	P
9	-	-	20.0	-	-	-	20.0	-
10	5.0	a tf	10.0	A P	5.0	tf	7.5	P
11	-	-	20.0	-	-	-	20.0	-
12	2.5	tf	10.0	A P	15.0	te	20.0	A ts
13	10.0	te	15.0	A D	12.5	te	15.0	D
14	3.5	a te	10.0	A P	7.5	D	7.5	D
15	-	-	20.0	-	-	-	20.0	-
16	3.5	te	10.0	A P	8.5	te	15.0	D
	Array A - Chronic 1				Array B - Chronic 2			
El.	Thresh	Mov	Max	Mov	Thresh	Mov	Max	Mov
1	-	-	20.0	-	7.5	tf	15.0	P
2	5.0	tf	20.0	P	10.0	tf	15.0	P
3	-	-	20.0	-	10.0	tf	20.0	P
4	20.0	tf	25.0	P	10.0	tf	20.0	P
5	10.0	tf	20.0	P	15.0	tf	20.0	P
6	10.0	tf	20.0	P	5.0	tf	10.0	P
7	8.5	tf	15.0	P	10.0	tf	20.0	P
8	11.0	tf	20.0	P	5.0	tf	10.0	P
9	-	-	20.0	-	3.0	d	10.0	D
10	-	-	20.0	-	-	-	20.0	-
11	-	-	20.0	-	-	-	20.0	-
12	10.0	tf	15.0	P	2.5	te*	10.0	D
13	15.0	tf	20.0	P	-	-	20.0	-
14	12.5	te	17.5	D	5.0	d	10.0	D
15	-	-	20.0	-	2.5	d	10.0	D
16	-	-	20.0	-	2.5	d	10.0	D

symbol	movement	symbol	movement
a A	Leg abduction	ts	Digit separation
p P	Plantar flexion	tf	Digit flexion
d D	Dorsiflexion	te	Digit extension
**	Movement seen in a single digit.		
lower	weak response	UPPER	strong response

crostimulator into a nerve cuff. Despite a multitude of steps required to design, fabricate, and test the WFMA, we have shown the feasibility of using this platform technology for numerous peripheral and central nervous system applications. The length and area of the electrodes can be chosen to optimize the particular desired stimulator use. In this study, these were chosen to accommodate the rodent sciatic nerve. As can be seen in Figure 6, the width of the nerve was less than the span of the WFMA electrodes. It is likely that this dimensional mismatch was responsible for the variations in electrode utilization, as supported by the comparisons in Table I for the three animals used for testing Array A. The in-vitro data shown in Figure 5 demonstrate the utility of the reverse telemetry WFMA capability. Being able to observe the shape of the waveforms yields valuable insight into the behavior of the electrodes while under constant-current pulsing. The Reference electrode shows the Counter electrode potential relative to the ASIC substrate and measures the 3.5V cathodic complicance voltage. With the Active

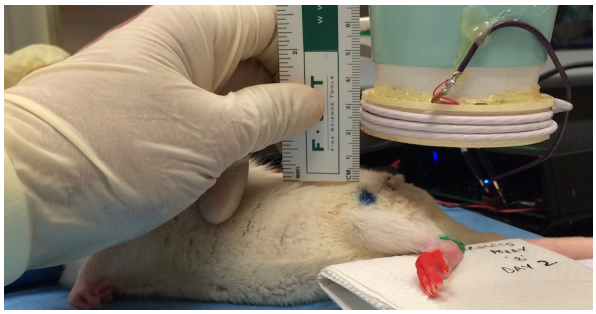

Fig. 7. Transmission of commands and reverse telemetry were possible at distances of up to 3cm (2cm away from the animals' skin).

electrode biased at 0.6V above Reference, a total compliance voltage of 4.1V is achieved. Lastly, the wireless transmission distance of 3cm is impressive, considering the small size of, and the weak inductive coupling to, the WFMA.

REFERENCES

[1] Ghovanloo, M; K Najafi, "A Modular 32-site wireless neural stimulation microsystem," IEEE Journal of Solid-State Circuits, vol. 39, no. 12, pp. 2457-2466, Dec 2004.

[2] Shuenn-Yuh Lee; Shyh-Chyang Lee, "An implantable wireless bidirectional communication microstimulator for neuromuscular stimulation," IEEE Transactions on Circuits and Systems I: Regular Papers, vol. 52, no. 12, pp. 2526-2538, Dec 2005.

[3] Thurgood, BK; DJ Warren, NM Ledbetter, GA Clark, RR Harrison, "A Wireless Integrated Circuit for 100-Channel Charge-Balanced Neural Stimulation," IEEE Transactions on Biomedical Circuits and Systems, vol. 3, no. 6, pp. 405-414, Dec 2009.

[4] Troyk, PR; T Bak, J Berg, D Bradley, S Cogan, R Erickson, et al., "A model for intracortical visual prosthesis research," Artificial Organs, vol. 27, pp. 1005-1015, Nov 2003.

[5] Troyk, PR; D Bradley, MJ Bak, S Cogan, R Erickson, Z Hu, C Kufta, D McCreery, E Schmidt, S Sung, V Towle, "Intracortical Visual Prosthesis Research - Approach and Progress," 27th Annual International Conference of the IEEE Engineering in Medicine and Biology Society, pp. 7376-7379, Jan 2006.

[6] Hu, Z; PR Troyk, GA DeMichele, K Kayvani, S Suh, "Intrinsic activation of iridium electrodes over a wireless link," 2012 Annual International Conference of the IEEE Engineering in Medicine and Biology Society, pp. 2788-2791, Aug 2012.

[7] Cogan, SF; PR Troyk, J Ehrlich, TD Plante, DE Detlefsen, "Potential-biased, asymmetric waveforms for charge-injection with activated iridium oxide (AIROF) neural stimulation electrodes," IEEE Transactions on Biomedical Engineering, vol. 53, pp. 327-332, Feb 2006.

[8] Troyk, PR; DE Detlefsen, GA DeMichele, "A Multifunctional Neural Electrode Stimulation ASIC using NeuroTalkTM Interface," 28th Annual International Conference of the IEEE Engineering in Medicine and Biology Society, pp. 2994-2997, Aug 2006.

[9] Rush, A; S Suh, PR Troyk, "An inductive link for an intracortical visual prosthesis," 5th International IEEE/EMBS Conference on Neural Engineering, pp. 503-506, Apr 2011.

[10] Troyk, PR; GA DeMichele, "Inductively-coupled power and data link for neural prostheses using a class-E oscillator and FSK modulation," 25th Annual International Conference of the IEEE Engineering in Medicine and Biology Society, pp. 3376-3379, Sep 2003.

[11] Suh, S; PR Troyk, Z Hu, "Accelerated-stress reliability evaluation for an encapsulated wireless cortical stimulator," 36th Annual International Conference of the IEEE Engineering in Medicine and Biology Society, pp. 442-445, Aug 2014.

[12] Musallam, S; MJ Bak, PR Troyk, RA Andersen, "A floating metal microelectrode array for chronic implantation," Journal of Neuroscience Methods, vol. 160, pp. 122-127, Feb 2007.

[13] Troyk, P; Z Hu, "Simplified Design Equations for Class-E Neural Prosthesis Transmitters," IEEE Transactions on Biomedical Engineering, vol. 60, no. 5, pp. 1414-1421, May 2013.